Nano Res. 2012, 5(11): 762–769
DOI 10.1007/s12274-012-0259-5
Research Article

ISSN 1998-0124
CN 11-5974/O4

Visible Light Active Pure Rutile TiO_2 Photoanodes with 100% Exposed Pyramid-Shaped (111) Surfaces

Xiaolu Liu[1], Haimin Zhang[1], Xiangdong Yao[2], Taicheng An[3], Porun Liu[1], Yun Wang[1], Feng Peng[4], Anthony R. Carroll[1], and Huijun Zhao[1] (✉)

[1] Centre for Clean Environment and Energy, and Griffith School of Environment, Griffith University, Gold Coast Campus, QLD 4222, Australia
[2] QLD Micro- and Nanotechnology Centre, Griffith University, Nathan Campus, QLD 4111, Australia
[3] State Key Laboratory of Organic Geochemistry, Guangzhou Institute of Geochemistry, Chinese Academy of Sciences, Guangzhou 510640, China
[4] School of Chemistry and Chemical Engineering, South China University of Technology, Guangzhou 510640, China

Received: 10 August 2012 / Revised: 31 August 2012 / Accepted: 9 September 2012

ABSTRACT

A pure rutile TiO_2 photoanode with 100% exposed pyramid-shaped (111) surfaces has been directly synthesized on a fluorine-doped tin oxide (FTO) conducting substrate via a facile one-pot hydrothermal method. The resulting rutile TiO_2 film on the FTO substrate possessed a film thickness of ca. 5 μm and showed good mechanical stability. After calcination at 450 °C for 2 h in argon (Ar), the fabricated rutile TiO_2 films with 100% exposed pyramid-shaped (111) surfaces were used as photoanodes, exhibiting excellent visible light photoelectrocatalytic activity toward oxidation of water and organics. The excellent visible light activity of the pure rutile TiO_2 film photoanode can be attributed to the Ti^{3+} doping in the bulk and high reactivity of the {111} crystal facets. Such a pure rutile TiO_2 film with highly reactive (111) surfaces is a promising material for visible light photocatalysis and solar energy conversion.

KEYWORDS

Rutile TiO_2, high energy {111} facets, hydrothermal synthesis, photoelectrocatalysis, visible light activity

1. Introduction

Titanium dioxide (TiO_2) materials with highly reactive crystal facets have aroused great interest because of their superior performance [1–11]. However, pure TiO_2 with its large band gap (3.2 eV for anatase) is not an ideal candidate for visible light applications. To improve the sunlight utilization efficiency, a variety of approaches has been developed to obtain visible light active TiO_2 including doping (e.g. N-doping), sensitization (e.g. with dyes) and surface hydrogenation [7, 12–14]. Surface hydrogenation approaches have been widely investigated to obtain reduced forms of TiO_2 (TiO_{2-x}) with Ti^{3+} or O vacancies to generate visible light activity [14, 15]. Nevertheless, the surface oxygen defects for reduced forms of TiO_2 are highly unstable in air due to the susceptibility of Ti^{3+} toward O_2 oxidation, affecting the practical use of such forms

Address correspondence to h.zhao@griffith.edu.au

of TiO_2 [16]. Recently, Feng et al. reported a visible light active TiO_2 with self-doped Ti^{3+} in the bulk that demonstrates a high visible light photocatalytic activity [17, 18]. Importantly, the Ti^{3+} sites formed in the bulk are found to be highly stable in air and water for repetitive use [17, 18]. However, only powder forms of products can be obtained by their method, which is disadvantageous for photoelectrocatalytic-based applications.

Anatase TiO_2 with exposed high energy facets such as {001} facets has been confirmed to have high photocatalytic activity [1, 3, 19]. For rutile TiO_2, studies have shown that high energy facets such as {111} facets possess superior activity in photocatalytic oxidation [5, 17, 20–22]. It has also been reported that the {111} and {110} facets of rutile TiO_2 usually act as oxidative and reductive sites to trap photoholes and electrons, resulting in oxidation and reduction occurring respectively on {111} and {110} facets [17, 22]. To date, few studies of visible light active rutile TiO_2 have been reported in the literature and little is known about such materials, especially their photoelectrocatalytic properties.

In this work, we report for the first time a facile one-pot hydrothermal method to directly grow visible light active rutile TiO_2 films with 100% exposed pyramid-shaped (111) surfaces on fluorine-doped tin oxide (FTO) substrates. After calcination at 450 ℃ in argon (Ar), the resultant rutile TiO_2 film can be directly used as a photoanode, having excellent photoelectrocatalytic activity toward water and glucose oxidation under visible light irradiation ($\lambda > 400$ nm). The presence of bulk Ti^{3+} enables the visible light absorption and improves the stability [17], while the 100% exposed high energy {111} facets promote the photocatalytic oxidation efficiency [20, 22]. This is the first time that the visible light photoelectrocatalytic activity of a pure rutile TiO_2 photoanode has been quantitatively characterized.

2. Experimental

2.1 Synthesis of rutile TiO_2 film

The visible light active pure rutile TiO_2 films with 100% exposed pyramid-shaped (111) surfaces on FTO conducting substrates were fabricated by a facile one-pot hydrothermal method. In a typical synthesis process, 0.04 g of titanium nitride (TiN, >95%, Aldrich) was added to a mixture containing 13.5 mL of high-purity deionized water (Millipore Corp., 18 MΩ·cm), 13.5 mL of concentrated hydrochloric acid (HCl, 32%, Sigma–Aldrich) and 3 mL of hydrogen peroxide (H_2O_2, 30%, Aldrich). After magnetically stirring for 60 s, the reaction solution was transferred into a Teflon-lined stainless steel autoclave (80 mL in volume). Before hydrothermal reaction, a piece of cleaned FTO conducting substrate (30 mm × 15 mm × 2 mm) was immersed into the above reaction solution with the conductive side facing up. The subsequent hydrothermal reaction was carried out at 200 ℃ for 24 h. After hydrothermal reaction, the autoclave was naturally cooled down to room temperature. The FTO conducting substrate was taken out, rinsed adequately with deionized water and allowed to dry in a nitrogen stream. The resulting materials were then calcined in a tube furnace at 450 ℃ for 2 h in argon (Ar) with a heating rate of 5 ℃/min. For comparison, the as-synthesized rutile TiO_2 film samples were also calcined at 450 ℃ for 2 h in air. A P25 photoanode was prepared by sol–gel and calcination methods.

2.2 Characterization

The structural characteristics of the samples were investigated by scanning electron microscopy (SEM, JSM-6300F), transmission electron microscopy (TEM, Philips F20), and X-ray diffraction (XRD, Shimadzu XRD-6000, equipped with graphite monochromated Cu Kα radiation). The chemical compositions of the samples were analyzed by X-ray photoelectron spectroscopy (XPS, Kratos Axis ULTRA incorporating a 165 mm hemispherical electron energy analyzer), and the UV–vis diffuse reflectance spectra of the samples were recorded on a Varian Cary 5E UV–vis–NIR spectrophotometer.

2.3 Photoelectrochemical measurements

The photoelectrochemical measurements were performed using a photoelectrochemical cell with a quartz window for illumination. A three-electrode mode, consisting of a TiO_2 nanostructured photoanode, a

saturated Ag/AgCl reference electrode and a platinum mesh counter electrode, was employed in the experiments. 0.10 mol/L $NaNO_3$ solution was used as supporting electrolyte. A voltammograph (CV-27, BAS) was used for the application of potential bias. Potential and current signals were recorded using a Macintosh (AD Instruments). The illuminated area of the photoanode was 0.785 cm^2. Illumination was carried out using a 150 W xenon arc lamp light source with focusing lenses (HF-200W-95, Beijing Optical Instruments). The wavelengths of incident light lower than 400 nm were cut off by a UV-400 filter. The light intensity of visible light was carefully measured with a visible-irradiance meter (Nova-Oriel, OPHIR). Mott–Schottky experiments of the photoanodes investigated were performed in 0.10 mol/L $NaNO_3$ solution under visible light illumination with light intensity of 500 mW/cm^2.

3. Results and discussion

Figure 1(a) shows typical X-ray diffraction (XRD) patterns of the as-synthesized sample, the samples calcined at 450 ℃ in air and Ar. The data confirm that all samples are tetragonal structured rutile TiO_2 with cell parameters of a = 4.584 Å and c = 2.953 Å (JCPDS No. 89-4920). The low magnification scanning electron microscopy (SEM) image of the calcined sample in Ar given in Fig. 1(b) reveals a uniform surface morphology with well-defined pyramid-shaped crystal facets. The high magnification SEM image (Fig. 1(c)) shows that the angle between the bottom and lateral edges of the pyramid crystal facet is 53.6°, matching closely to the theoretical value between the [110] and [011] directions for a tetragonal rutile TiO_2 [17]. The cross-sectional SEM image reveals a compactly packed nanorod-like array film structure ca. 5 μm in thickness, meaning 100% exposed pyramid-shaped crystal facets (Fig. 1(d)). To obtain more detailed structural information, transmission electron microscopy (TEM) analysis was performed (Fig. 1(e)). The selected area electron diffraction (SAED) and high-resolution TEM (HRTEM) image (insets in Fig. 1(e)) confirm the good single crystalline nature of the rutile TiO_2 structure. The SAED pattern reveals a preferred growth along the [001] direction. The HRTEM image confirms the fringe

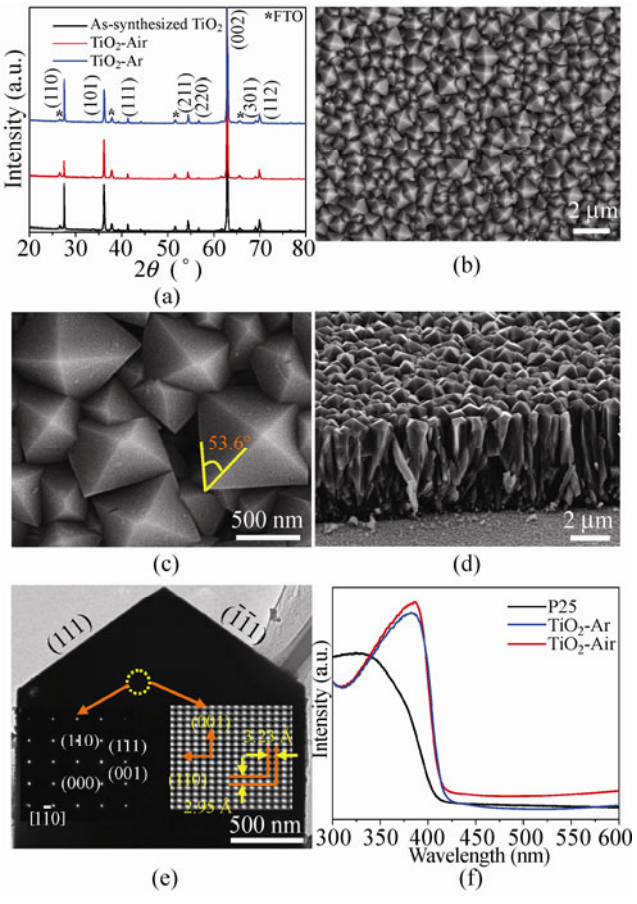

Figure 1 (a) XRD patterns of the as-synthesized TiO_2 product and calcined products in air and Ar. (b) and (c) Surface SEM images of the rutile TiO_2 film calcined in Ar. (d) Cross-sectional SEM image of the film. (e) TEM image of an individual rod-like structure; insets show the SAED pattern and HRTEM image. (f) UV–vis absorption spectra of the calcined samples in air and Ar and P25

spacings of 3.23 Å and 2.95 Å, which are consistent with the d values of the (110) and (001) planes, respectively, of the tetragonal rutile TiO_2 [17]. The above investigations confirm that the exposed pyramid-shaped crystal facets are {111} facets [17]. Figure 1(f) shows the UV–vis diffuse reflectance spectra of the rutile TiO_2 film samples annealed at 450 ℃ in Ar and air, and the commercial Degussa P25. It can be seen that the rutile TiO_2 film samples calcined in Ar and air exhibit similar UV–vis absorption spectra. In comparison to the commercial P25, obviously red-shifted absorption spectra were obtained from the calcined rutile TiO_2 film samples, suggesting a decreased band gap of {111} faceted rutile TiO_2, capable of absorbing visible light. A similar phenomenon

has been recently reported by Feng et al. [17]. Their experimental and theoretical calculation results revealed that the presence of Ti^{3+} in the bulk could create a vacancy band of electronic states below the conduction band (CB), responsible for the narrowed band gap and capability of visible light activity [17, 18].

In this work, the presence of H_2O_2 in the reaction solution was found to play a key role in the formation of high quality rutile TiO_2 films with exposed (111) surfaces on the FTO substrate (Fig. 2(a)). In the absence of H_2O_2, the formed film possessed very poor mechanical properties and weak adhesion to the substrate so that it could be easily broken down and peeled off the substrate (Fig. 2(b)). Under such conditions, the resultant film shows irregular surface morphologies with imperfect pyramidal crystal facets (Fig. 2(c)). The beneficial effect of H_2O_2 can be attributed to the formation of peroxotitanium complexes by Ti^{4+} reacting with H_2O_2 during the hydrothermal process to slow down the hydrolysis of the titanium precursor and favor the formation of {111} facets [3, 23].

A similar rutile TiO_2 structures with exposed {111} facets has been reported by Fujihara et al. [24]. However, their study only focused on the fabrication of the rutile TiO_2 rod structures without demonstrating the potential benefits of such high energy facets for visible light photocatalytic applications [24]. In this work, the pure rutile TiO_2 film photoanode with 100% exposed pyramid-shaped (111) surfaces was fabricated by annealing the as-synthesized rutile TiO_2 at 450 ℃ in Ar. The visible light photoelectrocatalytic activities

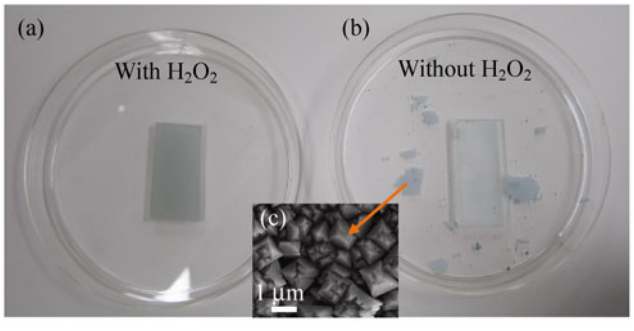

Figure 2 Optical photos of the obtained rutile TiO_2 film samples with (a) and without (b) H_2O_2 in the reaction solution. (c) Surface SEM image of the obtained rutile TiO_2 film without addition of H_2O_2 in the reaction solution. Materials were prepared with a hydrothermal reaction temperature of 200 ℃ and reaction time of 24 h

of the resultant photoanode were evaluated using water and glucose as the probe compounds under visible light irradiation ($\lambda > 400$ nm). Figure 3(a) shows the voltammograms of the photoanode in 0.10 mol/L $NaNO_3$ supporting electrolyte with and without visible light illumination. It can be seen that without the illumination, only a negligible dark current can be observed. For all cases with illumination, the photocurrents (I_{ph}) initially increase linearly with the applied potential bias due to the limitation of photoelectron transport within the rutile TiO_2 photocatalyst film [23, 25]. The photocurrents saturate at higher potentials (e.g. applied potential bias more positive than +0.22 V), owing to the limitation of the interfacial processes at the photocatalyst/solution interface [23, 25]. For all cases with visible light illumination, an increase in the light intensity leads to an increase in the saturated photocurrent, suggesting a good visible light activity of the photoanode toward water oxidation. Our previous studies have indicated that the magnitude of the saturated photocurrent represents the maximum rate of water oxidation under a given light intensity [23, 25]. Figures 3(b) and 3(c) show the transient photocurrent responses obtained at + 0.40 V (vs. Ag/AgCl) applied potential with different light intensities (φ) in 0.10 mol/L $NaNO_3$ solution and with 50 mmol/L added glucose, respectively. For all cases, an increase in the light intensity leads to an increase in the photocurrent. For a given light intensity, the corresponding photocurrent obtained in the presence of glucose is much higher than that obtained from just electrolyte solution, because the photocurrent obtained in the presence of glucose results from photoelectrocatalytic oxidation of both water and glucose [23, 25].

Figure 3(d) shows the plots of the steady-state photocurrent (I_{ph}) obtained from Figs. 3(b) and 3(c) against the visible light intensities (φ). Well-defined I_{ph}–φ linear relationships are obtained. The slope values of 0.073 and 0.104 μA/mW were obtained from oxidation of water (derived from Fig. 3(b)) and the combined water and glucose oxidations (derived from Fig. 3(c)), respectively. Under the given experimental conditions, the slope value of the I_{ph}–φ curve quantitatively represents the photoelectrocatalytic activity of the photoanode [23, 25]. The obtained slope ratio of 1.42 suggests a high visible light photoelectrocatalytic

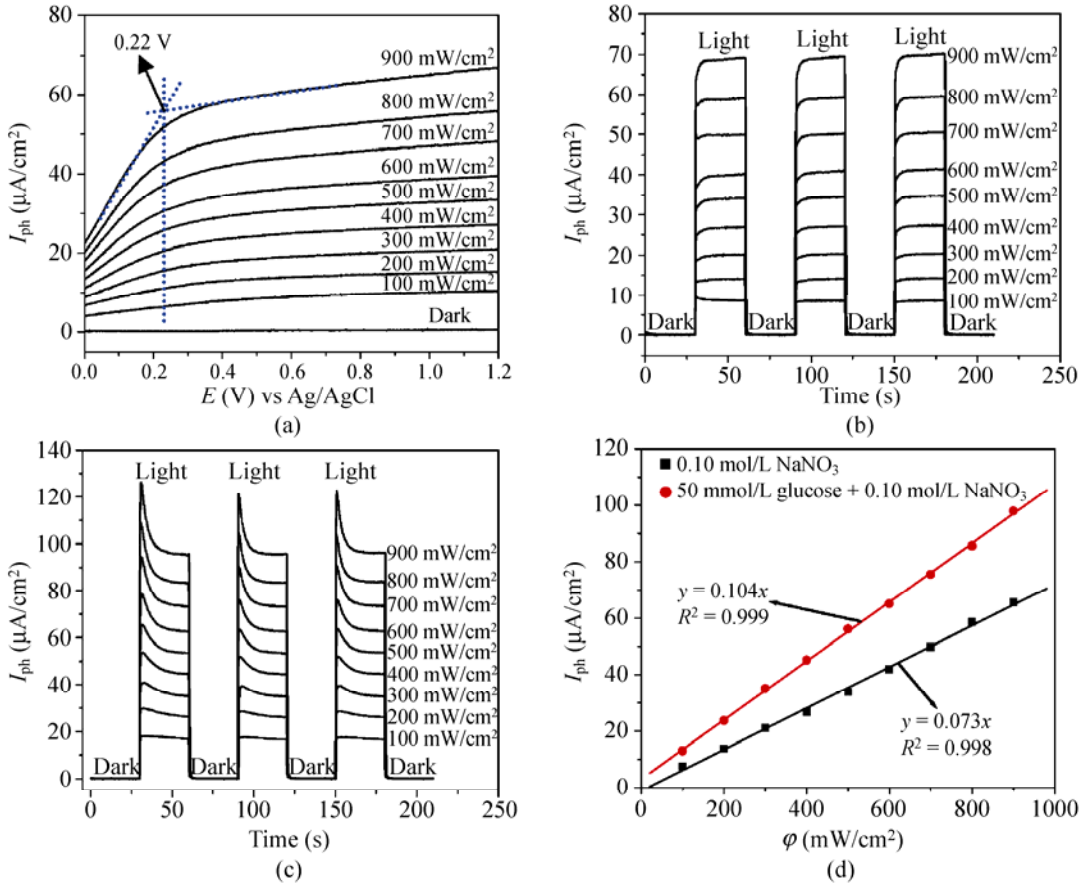

Figure 3 (a) Voltammograms of the photoanode obtained in 0.10 mol/L $NaNO_3$ solution under different light intensities. Transient photocurrent responses obtained at + 0.40 V applied potential with different light intensities in (b) 0.10 mol/L $NaNO_3$ solution and (c) with 50 mmol/L added glucose, respectively. (d) I_{ph}–φ relationships derived from Figs. 3(b) and 3(c)

activity toward glucose oxidation. Importantly, the photoanode displays a superior stability as no photoelectrocatalytic activity decay was observed after repeated photoelectrocatalytic cycles, attributed to the high stability of bulk doped Ti^{3+} [17, 18]. Recently, a similar rutile TiO_2 structure with exposed pyramid-shaped {111} crystal facets was reported by Feng et al. [17]. Their studies showed that the visible light activity originated from the Ti^{3+} doping in the bulk [17]. It is believed that the visible light activity in our materials may also be attributed to the presence of Ti^{3+} in the bulk of the rutile TiO_2 film.

In this work, TiN was used as titanium source. TiN as a precursor has been used to synthesize N-doped anatase TiO_2 nanosheets with exposed {001} facets [12]. The resulting product showed visible light activity due to N doping in the bulk TiO_2 [12]. In the previous study, two bonding states of nitrogen species were observed with N 1s binding energies of 399.5 and 401.0 eV [12]. However, in this work, the X-ray photoelectron spectra (XPS) confirmed the absence of N in all the investigated rutile TiO_2 film samples (Fig. S-1 in the Electronic Supplementary Material (ESM)). This indicates that the visible light activity of the rutile TiO_2 film does not originate from N doping. Also, the high-resolution XPS study confirms that no Ti^{3+} exists on the surface of the rutile TiO_2, as shown in Fig. 4(a). The above results suggest that the visible light activity of the obtained rutile TiO_2 film can be attributed to the presence of Ti^{3+} in the bulk TiO_2 rather on the surface [17, 18]. Figure 4(b) shows X-ray photoelectron valence band (VB) spectra of the rutile TiO_2 film calcined in Ar and commercial P25. It reveals the same VB maximum of ca. 1.96 eV for both samples,

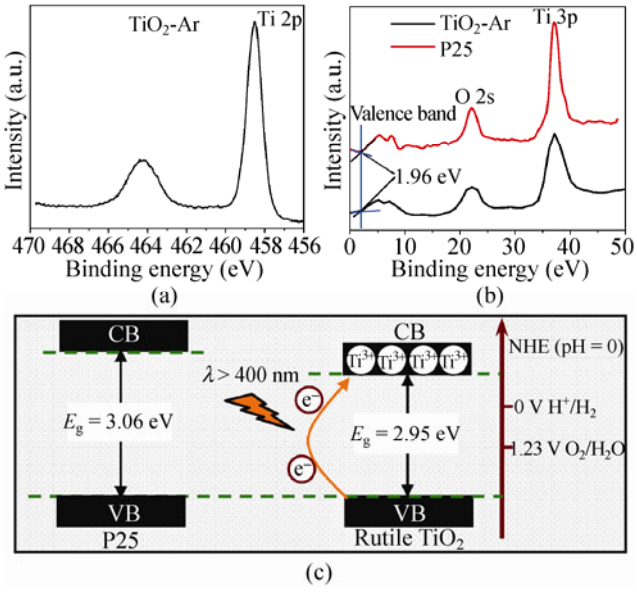

Figure 4 (a) High resolution XPS spectra of Ti 2p for the rutile TiO_2 sample. (b) XPS valence band spectra of the rutile TiO_2 and P25. (c) Determined valence band and conduction band edges of the rutile TiO_2 and P25

meaning that the valence band edge position of both samples is identical [23, 26]. However, compared to P25, the conduction band (CB) minimum of the rutile TiO_2 sample has positively shifted by ca. 0.11 eV, due to the presence of Ti^{3+} in the bulk (Fig. 4(c)) [17, 18].

For comparison, a P25 photoanode and the rutile TiO_2 film photoanode calcined at 450 ℃ in air were also prepared in this work. Figure 5(a) shows the voltammograms of the photoanodes calcined in Ar and air and the P25 photoanode in 0.10 mol/L $NaNO_3$ supporting electrolyte with and without visible light illumination. The photoelectrocatalytic experiment under visible light irradiation indicates that no photocurrent response is observed for the P25 photoanode due to its larger band gap (Fig. 5(a)). The photocurrent response of the photoanode calcined in air is almost ~2/3 of that of the photoanode calcined in Ar (Fig. 5(a)). This may be due to the oxidation of shallow doped Ti^{3+} by O_2 under high temperature, leading to a decrease in the Ti^{3+} concentration in the bulk, and a concomitant decrease in the number of visible light active sites and the photogenerated carrier concentration. Figure 5(b) shows Mott–Schottky plots of the rutile TiO_2 film photoanodes annealed at 450 ℃ in air (TiO_2-air) and Ar (TiO_2-Ar) under visible light irradiation (500 mW/cm^2). The slope of the tangent line in a Mott–Schottky plot is proportional to $1/N_D$ (where N_D is the number of donors) [27]. The slope of the plot for TiO_2-Ar is significantly lower than that for TiO_2-air, indicating a higher photogenerated carrier concentration in the TiO_2-Ar film. The higher carrier concentration in the TiO_2-Ar film means that more photoelectrons can be effectively transferred to the external circuit in the photoelectrocatalytic reaction, thus leading to higher photocurrent response.

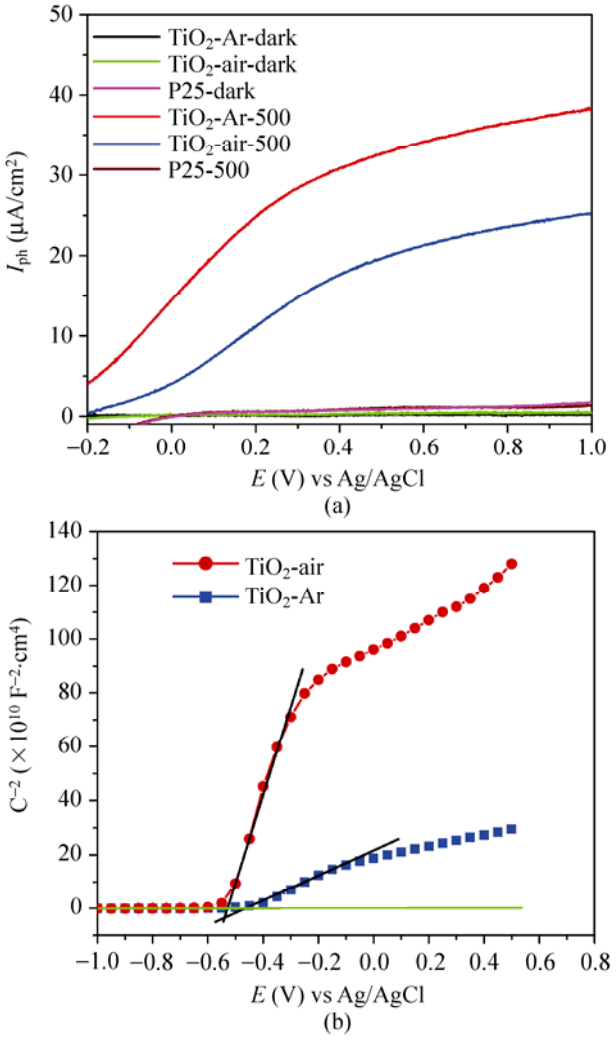

Figure 5 (a) Voltammograms obtained under a light intensity of 500 mW/cm^2 from rutile TiO_2 film photoanodes calcined at 450℃ for 2 h in air and Ar in 0.10 mol/L $NaNO_3$ solution. (b) Mott–Schottky plots of the photoanodes calcined at 450 ℃ for 2 h in air (TiO_2-air) and Ar (TiO_2-Ar). The experiments were performed in 0.10 mol/L $NaNO_3$ solution under visible light illumination with light intensity of 500 mW/cm^2

4. Conclusion

Visible light active rutile TiO_2 with 100% exposed pyramid-shaped (111) surfaces can be directly grown on a FTO substrate via a facile one-pot hydrothermal method. The photoanode prepared by annealing the as-synthesized rutile TiO_2 at 450 ℃ in Ar exhibits a superior visible light photoelectrocatalytic activity toward oxidation of water and glucose. It is believed that the superior stability and visible light activity are contributed by the bulk doped Ti^{3+} and the 100% exposed high energy {111} facets. The findings reported here suggest that other than elemental doping and sensitization, a visible light active pure TiO_2 can be synthesized by a self-doping approach.

Acknowledgements

This work was financially supported by the Australian Research Council Discovery Project.

Electronic Supplementary Material: Supplementary material is available in the online version of this article at http://dx.doi.org/10.1007/s12274-012-0259-5.

References

[1] Yang, H. G.; Sun, C. H.; Qiao, S. Z.; Zou, J.; Liu, G.; Smith, S. C.; Cheng, H. M.; Lu, G. Q. Anatase TiO_2 single crystals with a large percentage of reactive facets. *Nature* **2008**, *453*, 638–641.

[2] Yang, H. G.; Liu, G.; Qiao, S. Z.; Sun, C. H.; Jin, Y. G.; Smith, S. C.; Zou, J.; Cheng, H. M.; Lu, G. Q. Solvothermal synthesis and photoreactivity of anatase TiO_2 nanosheets with dominant {001} facets. *J. Am. Chem. Soc.* **2009**, *131*, 4078–4083.

[3] Liu, M.; Piao, L.; Zhao, L.; Ju, S.; Yan, Z.; He, T.; Zhou, C.; Wang, W. Anatase TiO_2 single crystals with exposed {001} and {110} facets: Facile synthesis and enhanced photocatalysis. *Chem. Commun.* **2010**, *46*, 1664–1666.

[4] Liu, G.; Sun, C.; Yang, H. G.; Smith, S. C.; Wang, L.; Lu, G. Q.; Cheng, H. M. Nanosized anatase TiO_2 single crystals for enhanced photocatalytic activity. *Chem. Commun.* **2010**, *46*, 755–757.

[5] Sun, L.; Qin, Y.; Cao, Q.; Hu, B.; Huang, Z.; Ye, L.; Tang, X. Novel photocatalytic antibacterial activity of TiO_2 microspheres exposing 100% reactive {111} facets. *Chem. Commun.* **2011**, *47*, 12628–12630.

[6] Chen, J. S.; Tan, Y. L.; Li, C. M.; Cheah, Y. L.; Luan, D.; Madhavi, S.; Boey, F. Y. C.; Archer, L. A.; Lou, X. W. Constructing hierarchical spheres from large ultrathin anatase TiO_2 nanosheets with nearly 100% exposed (001) facets for fast reversible lithium storage. *J. Am. Chem. Soc.* **2010**, *132*, 6124–6130.

[7] Zhang, H.; Han, Y.; Liu, X.; Liu, P.; Yu, H.; Zhang, S.; Yao, X.; Zhao, H. Anatase TiO_2 microspheres with exposed mirror-like plane {001} facets for high performance dye-sensitized solar cells (DSSCs). *Chem. Commun.* **2010**, *46*, 8395–8397.

[8] Zhang, H.; Liu, P.; Li, F.; Liu, H.; Wang, Y.; Zhang, S.; Guo, M.; Cheng, H.; Zhao, H. Facile fabrication of anatase TiO_2 microspheres on solid substrates and surface crystal facet transformation from {001} to {101}. *Chem.—Eur. J.* **2011**, *17*, 5949–5957.

[9] Zheng, Z.; Huang, B.; Qin, X.; Zhang, X.; Dai, Y.; Jiang, M.; Wang, P.; Whangbo, M. H. Highly efficient photocatalyst: TiO_2 microspheres produced from TiO_2 nanosheets with a high percentage of reactive {001} Facets. *Chem.—Eur. J.* **2009**, *15*, 12576–12579.

[10] Chen, X.; Shen, S.; Guo, L.; Mao, S. S. Semiconductor-based photocatalytic hydrogen generation. *Chem. Rev.* **2010**, *110*, 6503–6570.

[11] Shen, S.; Shi, J.; Guo, P.; Guo, L. Visible-light-driven photocatalytic water splitting on nanostructured semiconducting materials. *Int. J. Nanotechnol.* **2011**, *8*, 523–591.

[12] Liu, G.; Yang, H. G.; Wang, X.; Cheng, L.; Pan, J.; Lu, G. Q.; Cheng, H. M. Visible light responsive nitrogen doped anatase TiO_2 sheets with dominant {001} facets derived from TiN. *J. Am. Chem. Soc.* **2009**, *131*, 12868–12869.

[13] Santra, P. K.; Kamat, P. V. Mn-doped quantum dot sensitized solar cells: A strategy to boost efficiency over 5%. *J. Am. Chem. Soc.* **2012**, *134*, 2508–2511.

[14] Zheng, Z.; Huang, B.; Lu, J.; Wang, Z.; Qin, X.; Zhang, X.; Dai, Y.; Whangbo, M. H. Hydrogenated titania: Synergy of surface modification and morphology improvement for enhanced photocatalytic activity. *Chem. Commun.* **2012**, *48*, 5733–5735.

[15] Chen, X.; Liu, L.; Yu, P. Y.; Mao, S. S. Increasing solar absorption for photocatalysis with black hydrogenated titanium dioxide nanocrystals. *Science* **2011**, *331*, 746–750.

[16] Teleki, A.; Pratsinis, S. E. Blue nano titania made in diffusion flames. *Phys. Chem. Chem. Phys.* **2009**, *11*, 3742–3747.

[17] Zuo, F.; Bozhilov, K.; Dillon, R. J.; Wang, L.; Smith, P.; Zhao, X.; Bardeen, C.; Feng, P. Active facets on titanium(Ⅲ)-doped TiO_2: An effective strategy to improve the visible-light photocatalytic activity. *Angew. Chem. Int. Ed.* **2012**, *51*, 6223–6226.

[18] Zuo, F.; Wang, L.; Wu, T.; Zhang, Z.; Borchardt, D.; Feng, P. Self-doped Ti^{3+} enhanced photocatalyst for hydrogen production under visible light. *J. Am. Chem. Soc.* **2010**, *132*, 11856–11857.

[19] Yang, W.; Wan, F.; Wang, Y.; Jiang, C. Achievement of 6.03% conversion efficiency of dye-sensitized solar cells with single-crystalline rutile TiO_2 nanorod photoanode. *Appl. Phys. Lett.* **2009**, *95*, 133121.

[20] Oliver, P. M.; Watson, G. W.; Kelsey, E. T.; Parker, S. C. Atomistic simulation of the surface structure of the TiO_2 polymorphs rutile and anatase. *J. Mater. Chem.* **1997**, *7*, 563–568.

[21] Zhen, C.; Liu, G.; Cheng, H. -M. A film of rutile TiO_2 pillars with well-developed facets on an α-Ti substrate as a photoelectrode for improved water splitting. *Nanoscale* **2012**, *4*, 3871–3874.

[22] Murakami, N.; Ono, A.; Nakamura, M.; Tsubota, T.; Ohno, T. Development of a visible-light-responsive rutile rod by site-selective modification of iron(Ⅲ) ion on {111} exposed crystal faces for catalytic photodegradation of pollutants. *Appl. Catal. B: Environ.* **2010**, *97*, 115–119.

[23] Zhang, H.; Liu, X.; Li, Y.; Sun, Q.; Wang, Y.; Wood, B. J.; Liu, P.; Yang, D.; Zhao, H. Vertically aligned nanorod-like rutile TiO_2 single crystal nanowire bundles with superior electron transport and photoelectrocatalytic properties. *J. Mater. Chem.* **2012**, *22*, 2465–2472.

[24] Kakiuchi, K.; Hosono, E.; Imai, H.; Kimura, T.; Fujihara, S. {111}-faceting of low-temperature processed rutile TiO_2 rods. *J. Cryst. Growth* **2006**, *293*, 541–545.

[25] Jiang, D.; Zhao, H.; Zhang, S.; John, R. Characterization of photoelectrocatalytic processes at nanoporous TiO_2 film electrodes: Photocatalytic oxidation of glucose. *J. Phys. Chem. B* **2003**, *107*, 12774–12780.

[26] Pan, J.; Liu, G.; Lu, G. Q.; Cheng, H. M. On the true photoreactivity order of {001}, {010}, and {101} facets of anatase TiO_2 crystals. *Angew. Chem., Int. Ed.* **2011**, *50*, 2133–2137.

[27] Spadavecchia, F.; Cappelletti, G.; Ardizzone, S.; Ceotto, M.; Falciola, L. Electronic structure of pure and N-doped TiO_2 nanocrystals by electrochemical experiments and first principles calculations. *J. Phys. Chem. C* **2011**, *115*, 6381–6391.